

# Neutrino mass model with a modular $S_4$ symmetry

Hiroshi Okada<sup>1,\*</sup> and Yuta Orikasa<sup>2,†</sup>

<sup>1</sup>*Asia Pacific Center for Theoretical Physics (APCTP) - Headquarters San 31,  
Hyoja-dong, Nam-gu, Pohang 790-784, Korea*

<sup>2</sup>*Institute of Experimental and Applied Physics,  
Czech Technical University in Prague,*

*Husova 240/5, 110 00 Prague 1, Czech Republic*

(Dated: December 15, 2021)

## Abstract

We propose a predictive lepton model under a modular  $S_4$  symmetry, where the neutrino mass matrix arises from a radiative seesaw at one-loop level. The tree-level mass matrix is forbidden by well-assigned modular weights, which also play an important role in stabilizing dark matter candidate due to a remnant  $Z_2$  symmetry even after breaking the modular symmetry. Supposing three families of the Majorana neutrinos, right-handed charged-leptons and left-handed charged-leptons to be embedded respectively into singlet, doublet, and triplet under  $S_4$ , we obtain the predictive mass matrices in the normal hierarchy. Then, we show our numerical results such as phases, mixings, and neutrino masses, applying  $\chi^2$  analysis. We also demonstrate two sample points, imposing on minimizing  $\chi^2$  and best fit value of  $\delta_{CP}^\ell$  of  $195^\circ$ .

---

\*Electronic address: hiroshi.okada@apctp.org

†Electronic address: Yuta.Orikasa@utef.cvut.cz

## I. INTRODUCTION

Neutrino and dark matter (DM) physics are big issues to be solved beyond the standard model (SM), even though SM successfully describes a lot of phenomenologies in high energy physics. Radiative seesaw models are one of the attractive scenarios not only to explain both but also make a correlation between them. The first approach is achieved by Ref. [1], in which neutrino mass matrix is given at one-loop level, and a Majorana fermion DM or an inert scalar DM is included in the neutrino mass loop. It is also an important issue to resolve the flavor puzzles such as lepton flavor violations (LFVs),  $Z$  boson decays, flavor changing neutral currents enlightened by a lot of experimental results. These issues often arise from rather large Yukawa couplings that frequently appear on the radiative seesaw models, even though it also depends on structures of Yukawa matrices. If there exists a flavor symmetry such that their matrices are uniquely determined, it might provide powerful hints to the flavor physics.

Recently, modular flavor symmetries have been proposed [2, 3] to provide more predictions to the quark and lepton sector due to Yukawa couplings with a representation of a group. Their typical groups are found in basis of the  $A_4$  modular group [3–13],  $S_3$  [14–17],  $S_4$  [18–20],  $A_5$  [21, 22], larger groups [23, 24], multiple modular symmetries [25], and double covering of  $A_4$  [26] in which masses, mixings, and CP phases for quark and lepton are predicted.<sup>1</sup> Also, a systematic approach to understand the origin of CP transformations has been recently achieved by ref. [35].

In this paper, we introduce a modular  $S_4$  symmetry in the lepton sector, and the neutrino mass matrix is arisen via radiative seesaw at one-loop level. Supposing three families of the Majorana neutrinos, right-handed charged-leptons and left-handed charged-leptons to be embedded respectively into singlet, doublet, and triplet under  $S_4$ , we obtain the predictive mass matrices. Then, we show our numerical results such as phases, mixings, and neutrino masses, applying  $\chi^2$  analysis. Instead of an additional symmetry such as  $Z_2$  to stabilize DM, the model has a remnant symmetry of modular symmetry. This is why we have an appropriate DM candidate.

This paper is organized as follows. In Sec. II, we explain our model and formulate mass

---

<sup>1</sup> Several reviews are helpful to understand the whole idea [27–34].

	Fermions					Bosons	
	$\bar{L}_{L_{e,\mu,\tau}}$	$e_{R_e}$	$\ell_R \equiv (e_{R_\mu}, e_{R_\tau})^T$	$N_R \equiv (N_{R_1}, N_{R_2})^T$	$N_{R_3}$	$H$	$\eta^*$
$SU(2)_L$	<b>2</b>	<b>1</b>	<b>1</b>	<b>1</b>	<b>1</b>	<b>2</b>	<b>2</b>
$U(1)_Y$	$\frac{1}{2}$	-1	-1	0	0	$\frac{1}{2}$	$-\frac{1}{2}$
$S_4$	<b>3</b>	1	2	2	1	1	1
$-k$	-2	-2	-2	-1	-1	0	-3

TABLE I: Field contents of fermions and bosons and their charge assignments under  $SU(2)_L \times U(1)_Y \times S_4$  in the lepton and boson sector, where  $-k$  is the number of modular weight and the quark sector is the same as the SM.

	Couplings						
	$Y_2^{(2)}$	$Y_3^{(4)}$	$Y_{3'}^{(4)}$	$Y_1^{(6)}$	$Y_3^{(6)}$	$Y_{3'_1}^{(6)}$	$Y_{3'_2}^{(6)}$
$S_4$	<b>2</b>	<b>3</b>	<b>3'</b>	<b>1</b>	<b>3</b>	<b>3'</b>	<b>3'</b>
$-k$	2	4	4	6	6	6	6

TABLE II: Modular  $S_4$  representations for Yukawa couplings.

matrices, LFVs, and so on under the modular  $S_4$  symmetry. Then, we show numerical analyses for normal hierarchy (NH) and inverted hierarchy (IH) and discuss our predictions. We summarize and conclude in Sec. III. In appendix, we note the correspondence between confidence level(CL) and  $\chi^2$ , depending on the number of degrees of freedom for observables.

## II. MODEL

Here, we describe our scenario based on Ma model, where field contents are exactly the same as Ma model [1]. We introduce the Majorana fermions to be embedded into singlet and doublet under  $S_4$  and scalar bosons to be embedded into doublet under  $SU(2)_L$ . The singlet right-handed fermion is required because the neutrino oscillation data can't be explained in the model without singlet fermion. The  $S_4$  representation and modular weight are given by Tab. I, while the ones of Yukawa couplings are given by Tab. II. The

model has a remnant  $Z_2$  symmetry. Particles with odd modular weight have odd parity and particles with even modular weight have even parity. Under these symmetries, one writes renormalizable Lagrangian as follows:

$$\begin{aligned}
-\mathcal{L}_{Lepton} \supset & \alpha_\ell(Y_{\mathbf{3}}^{(4)} \otimes \bar{L}_L \otimes e_R)_1 H + \beta_\ell(Y_{\mathbf{3}}^{(4)} \otimes \bar{L}_L \otimes \ell_R)_1 H + \gamma_\ell(Y_{\mathbf{3}'}^{(4)} \otimes \bar{L}_L \otimes \ell_R)_1 H \\
& + \alpha_\eta(Y_{\mathbf{3}}^{(6)} \otimes \bar{L}_L \otimes N_R)_1 \tilde{\eta} + \left( (\beta_{\eta_1} Y_{\mathbf{3}'_1}^{(6)} + \beta_{\eta_2} Y_{\mathbf{3}'_2}^{(6)}) \otimes \bar{L}_L \otimes N_R \right)_1 \tilde{\eta} + \gamma_\eta(Y_{\mathbf{3}}^{(6)} \otimes \bar{L}_L \otimes N_{R_3})_1 \tilde{\eta} \\
& + M_0(Y_{\mathbf{2}}^{(2)} \otimes \bar{N}_R^C \otimes N_R)_1 + M_1(Y_{\mathbf{2}}^{(2)} \otimes \bar{N}_R^C \otimes N_{R_3})_1 + \text{h.c.}, \tag{II.1}
\end{aligned}$$

where  $\tilde{\eta} \equiv i\sigma_2 \eta^*$ ,  $\sigma_2$  being the second Pauli matrix.

The modular forms with the lowest weight 2 are given by  $Y_{\mathbf{2}}^{(2)} \equiv [y_1, y_2]^T$  and they respectively transform as a doublet and a triplet under  $S_4$  that are written in terms of Dedekind eta-function  $\eta(\tau)$  and its derivative [39]:

$$\begin{aligned}
y_1(\tau) &= \frac{i}{8} \left( 8 \frac{\eta'(\tau + \frac{1}{2})}{\eta(\tau + \frac{1}{2})} + 32 \frac{\eta'(4\tau)}{\eta(4\tau)} - \frac{\eta'(\frac{\tau}{4})}{\eta(\frac{\tau}{4})} - \frac{\eta'(\frac{\tau+1}{4})}{\eta(\frac{\tau+1}{4})} - \frac{\eta'(\frac{\tau+2}{4})}{\eta(\frac{\tau+2}{4})} - \frac{\eta'(\frac{\tau+3}{4})}{\eta(\frac{\tau+3}{4})} \right), \\
y_2(\tau) &= \frac{i\sqrt{3}}{8} \left( \frac{\eta'(\frac{\tau}{4})}{\eta(\frac{\tau}{4})} - \frac{\eta'(\frac{\tau+1}{4})}{\eta(\frac{\tau+1}{4})} + \frac{\eta'(\frac{\tau+2}{4})}{\eta(\frac{\tau+2}{4})} - \frac{\eta'(\frac{\tau+3}{4})}{\eta(\frac{\tau+3}{4})} \right) \\
y_3(\tau) &= i \left( \frac{\eta'(\tau + \frac{1}{2})}{\eta(\tau + \frac{1}{2})} - 4 \frac{\eta'(4\tau)}{\eta(4\tau)} \right), \\
y_4(\tau) &= \frac{i}{4\sqrt{2}} \left( -\frac{\eta'(\frac{\tau}{4})}{\eta(\frac{\tau}{4})} + i \frac{\eta'(\frac{\tau+1}{4})}{\eta(\frac{\tau+1}{4})} + \frac{\eta'(\frac{\tau+2}{4})}{\eta(\frac{\tau+2}{4})} - i \frac{\eta'(\frac{\tau+3}{4})}{\eta(\frac{\tau+3}{4})} \right), \\
y_5(\tau) &= \frac{i}{4\sqrt{2}} \left( -\frac{\eta'(\frac{\tau}{4})}{\eta(\frac{\tau}{4})} - i \frac{\eta'(\frac{\tau+1}{4})}{\eta(\frac{\tau+1}{4})} + \frac{\eta'(\frac{\tau+2}{4})}{\eta(\frac{\tau+2}{4})} + i \frac{\eta'(\frac{\tau+3}{4})}{\eta(\frac{\tau+3}{4})} \right). \tag{II.2}
\end{aligned}$$

Then, higher weights are constructed by multiplication rules of  $S_4$ , and one finds the following couplings:

$$\begin{aligned}
Y_{\mathbf{3}}^{(4)} &= \begin{bmatrix} -2y_2y_3 \\ \sqrt{3}y_1y_5 + y_2y_4 \\ \sqrt{3}y_1y_4 + y_2y_5 \end{bmatrix}, \quad Y_{\mathbf{3}'}^{(4)} = \begin{bmatrix} 2y_1y_3 \\ \sqrt{3}y_2y_5 - y_1y_4 \\ \sqrt{3}y_2y_4 - y_1y_5 \end{bmatrix}, \tag{II.3} \\
Y_{\mathbf{3}}^{(6)} &= \begin{bmatrix} y_1(y_4^2 - y_5^2) \\ y_3(y_1y_5 + \sqrt{3}y_2y_4) \\ -y_3(y_1y_4 + \sqrt{3}y_2y_5) \end{bmatrix}, \quad Y_{\mathbf{3}'_1}^{(6)} = (y_1^2 + y_2^2) \begin{bmatrix} y_3 \\ y_4 \\ y_5 \end{bmatrix}, \quad Y_{\mathbf{3}'_2}^{(6)} = \begin{bmatrix} y_2(y_5^2 - y_4^2) \\ y_3(y_2y_5 - \sqrt{3}y_1y_4) \\ y_3(y_2y_4 - \sqrt{3}y_1y_5) \end{bmatrix}. \tag{II.4}
\end{aligned}$$

After the electroweak spontaneous symmetry breaking, the charged-lepton mass matrix

is given by

$$m_\ell = \frac{v_H}{\sqrt{2}} \begin{bmatrix} \alpha_\ell Y_1 & \beta_\ell Y_1 & -\gamma_\ell Y_1' \\ \alpha_\ell Y_3 & -\frac{1}{2}\beta_\ell Y_3 + \frac{\sqrt{3}}{2}\gamma_\ell Y_2' & \frac{\sqrt{3}}{2}\beta_\ell Y_2 + \frac{1}{2}\gamma_\ell Y_3' \\ \alpha_\ell Y_2 & -\frac{1}{2}\beta_\ell Y_2 + \frac{\sqrt{3}}{2}\gamma_\ell Y_3' & \frac{\sqrt{3}}{2}\beta_\ell Y_3 + \frac{1}{2}\gamma_\ell Y_2' \end{bmatrix}, \quad (\text{II.5})$$

where  $\langle H \rangle \equiv [0, v_H/\sqrt{2}]^T$ ,  $Y_3^{(4)} \equiv [Y_1, Y_2, Y_3]^T$ , and  $Y_{3'}^{(4)} \equiv [Y_1', Y_2', Y_3']^T$ . Then the charged-lepton mass eigenstate can be found by  $|D_\ell|^2 \equiv V_{eL} m_\ell m_\ell^\dagger V_{eL}^\dagger$ . In our numerical analysis below, we fix the free parameters  $\alpha_\ell, \beta_\ell, \gamma_\ell$  to fit the three charged-lepton masses after giving all the numerical values, by applying the relations:

$$\text{Tr}[m_\ell m_\ell^\dagger] = |m_e|^2 + |m_\mu|^2 + |m_\tau|^2, \quad (\text{II.6})$$

$$\text{Det}[m_\ell m_\ell^\dagger] = |m_e|^2 |m_\mu|^2 |m_\tau|^2, \quad (\text{II.7})$$

$$(\text{Tr}[m_\ell m_\ell^\dagger])^2 - \text{Tr}[(m_\ell m_\ell^\dagger)^2] = 2(|m_e|^2 |m_\mu|^2 + |m_\mu|^2 |m_\tau|^2 + |m_e|^2 |m_\tau|^2). \quad (\text{II.8})$$

The right-handed neutrino mass matrix is given by

$$\mathcal{M}_N = M_0 \begin{bmatrix} -y_1 & y_2 & 0 \\ y_2 & y_1 & 0 \\ 0 & 0 & 0 \end{bmatrix} + M_1 \begin{bmatrix} 0 & 0 & y_1 \\ 0 & 0 & y_2 \\ y_1 & y_2 & 0 \end{bmatrix}. \quad (\text{II.9})$$

The heavy Majorana mass matrix is diagonalized by a unitary matrix  $V$  as follows:  $D_N \equiv V^* \mathcal{M}_N V^\dagger$ , where  $N_R \equiv V^\dagger \psi_R$ ,  $\psi_R$  being mass eigenstate.

The Dirac Yukawa matrix is given by

$$y_\eta = \begin{bmatrix} \alpha_\eta Y_1^6 & -\beta_{\eta_1} Y_1'^6 - \beta_{\eta_2} Y_1''6 & \gamma_\eta Y_1^6 \\ -\frac{1}{2}\alpha_\eta Y_3^6 + \frac{\sqrt{3}}{2}(\beta_{\eta_1} Y_2''6 + \beta_{\eta_2} Y_2''6) & \frac{\sqrt{3}}{2}\alpha_\eta Y_2 + \frac{\sqrt{1}}{2}(\beta_{\eta_1} Y_3''6 + \beta_{\eta_2} Y_3''6) & \gamma_\eta Y_3^6 \\ -\frac{1}{2}\alpha_\eta Y_2 + \frac{\sqrt{3}}{2}(\beta_{\eta_1} Y_3''6 + \beta_{\eta_2} Y_3''6) & \frac{\sqrt{3}}{2}\alpha_\eta Y_3^6 + \frac{\sqrt{1}}{2}(\beta_{\eta_1} Y_2''6 + \beta_{\eta_2} Y_2''6) & \gamma_\eta Y_2^6 \end{bmatrix}, \quad (\text{II.10})$$

where  $Y_3^{(6)} \equiv [Y_1^6, Y_2^6, Y_3^6]^T$ ,  $Y_{3_1}^{(6)} \equiv [Y_1'^6, Y_2'^6, Y_3'^6]^T$  and  $Y_{3_2}^{(6)} \equiv [Y_1''6, Y_2''6, Y_3''6]^T$ .

*Scalar potential* is given by

$$\begin{aligned} \mathcal{V} = & -\mu_H^2 |H|^2 + \mu_\eta^2 |\eta|^2 + \lambda_H |H|^4 + \lambda_\eta |\eta|^4 + \lambda_{H\eta} |H|^2 |\eta|^2 \\ & + \lambda'_{H\eta} |H^\dagger \eta|^2 + \frac{1}{2} \lambda''_{H\eta} [(H^\dagger \eta)^2 + \text{h.c.}], \end{aligned} \quad (\text{II.11})$$

where  $\lambda''_{H\eta}$  includes  $Y_1^{(6)}$  factor and  $\mu_\eta^2, \lambda_\eta, \lambda_{H\eta}, \lambda'_{H\eta}$  include  $1/(-i\tau + i\bar{\tau})^n$  factor. Scalar masses are given by

$$m_h^2 = 2\lambda_H v^2, \quad (\text{II.12})$$

$$m_R^2 = \mu_\eta^2 + \frac{1}{2} (\lambda_{H\eta} + \lambda'_{H\eta} + \lambda''_{H\eta}) v_H^2, \quad (\text{II.13})$$

$$m_I^2 = \mu_\eta^2 + \frac{1}{2} (\lambda_{H\eta} + \lambda'_{H\eta} - \lambda''_{H\eta}) v_H^2, \quad (\text{II.14})$$

$$m_{\eta^\pm}^2 = \mu_\eta^2 + \frac{1}{2} \lambda_{H\eta} v_H^2, \quad (\text{II.15})$$

where  $m_{R(I)}$  is a mass of the real (imaginary) component of  $\eta^0$ .

*Lepton flavor violations* also arise from  $y_\eta$  as [40, 41]

$$\text{BR}(\ell_i \rightarrow \ell_j \gamma) \approx \frac{48\pi^3 \alpha_{em} C_{ij}}{G_F^2 (4\pi)^4} \left| \sum_{\alpha=1}^3 Y_{\eta j \alpha} Y_{\eta \alpha i}^\dagger F(D_{N_\alpha}, m_{\eta^\pm}) \right|^2, \quad (\text{II.16})$$

$$F(m_a, m_b) \approx \frac{2m_a^6 + 3m_a^4 m_b^2 - 6m_a^2 m_b^4 + m_b^6 + 12m_a^4 m_b^2 \ln\left(\frac{m_b}{m_a}\right)}{12(m_a^2 - m_b^2)^4}, \quad (\text{II.17})$$

where  $Y_\eta \equiv y_\eta V^\dagger$   $C_{21} = 1$ ,  $C_{31} = 0.1784$ ,  $C_{32} = 0.1736$ ,  $\alpha_{em}(m_Z) = 1/128.9$ , and  $G_F = 1.166 \times 10^{-5} \text{ GeV}^{-2}$ . The experimental upper bounds are given by [42–44]

$$\text{BR}(\mu \rightarrow e \gamma) \lesssim 4.2 \times 10^{-13}, \quad \text{BR}(\tau \rightarrow e \gamma) \lesssim 3.3 \times 10^{-8}, \quad \text{BR}(\tau \rightarrow \mu \gamma) \lesssim 4.4 \times 10^{-8}, \quad (\text{II.18})$$

which will be imposed in our numerical calculation.

*Neutrino mass matrix* is given by a combination of canonical seesaw at tree-level and radiative seesaw at one-loop level by

$$\begin{aligned} m_{\nu_{ij}} &= \sum_{\alpha=1}^3 \left[ \frac{Y_{\eta i \alpha} M_{N_\alpha} Y_{\eta \alpha j}^T}{2(4\pi)^2} \left( \frac{m_R^2}{m_R^2 - M_{N_\alpha}^2} \ln \left[ \frac{m_R^2}{M_{N_\alpha}^2} \right] - \frac{m_I^2}{m_I^2 - M_{N_\alpha}^2} \ln \left[ \frac{m_I^2}{M_{N_\alpha}^2} \right] \right) \right] \\ &\simeq \frac{\lambda''_{H\eta} v_H^2}{2(4\pi)^2} \sum_{\alpha=1}^3 \frac{Y_{\eta i \alpha} M_{N_\alpha} Y_{\eta \alpha j}^T}{m_0^2 - M_{N_\alpha}^2} \left[ 1 - \frac{M_{N_\alpha}^2}{m_0^2 - M_{N_\alpha}^2} \ln \frac{m_0^2}{M_{N_\alpha}^2} \right], \end{aligned} \quad (\text{II.19})$$

where we assume to be  $\lambda''_{H\eta} v_H^2 = m_R^2 - m_I^2 \ll m_0^2 \equiv (m_R^2 + m_I^2)/2$  in the above second line. The neutrino mass matrix is diagonalized by a unitary matrix  $U_\nu$  as  $U_\nu m_\nu U_\nu^T = \text{diag}(m_{\nu_1}, m_{\nu_2}, m_{\nu_3}) \equiv D_\nu$ , where  $\text{Tr}[D_\nu] \lesssim 0.12 \text{ eV}$  is given by the recent cosmological data [45, 46]. The two mass squared differences are also measure by experiments and they are defined by

$$\text{NH} : \Delta m_{\text{sol}}^2 = m_{\nu_2}^2 - m_{\nu_1}^2, \quad \Delta m_{\text{atm}}^2 = m_{\nu_3}^2 - m_{\nu_1}^2, \quad (\text{II.20})$$

$$\text{IH} : \Delta m_{\text{sol}}^2 = m_{\nu_2}^2 - m_{\nu_1}^2, \quad \Delta m_{\text{atm}}^2 = m_{\nu_2}^2 - m_{\nu_3}^2. \quad (\text{II.21})$$

We use  $\lambda''_{H\eta}$  given by the following relation:

$$\lambda''_{H\eta} = \sqrt{\frac{\Delta m_{\text{sol}}^2}{\tilde{m}_{\nu_2}^2 - \tilde{m}_{\nu_1}^2}}, \quad (\text{II.22})$$

where  $\tilde{m}_{\nu_i} \equiv m_{\nu_i}/\lambda''_{H\eta}$ . Then, one finds  $U_{PMNS} = V_{eL}^\dagger U_\nu$ . Mixing angles are given in terms of the component of  $U_{PMNS}$  as follows:

$$\sin^2 \theta_{13} = |(U_{PMNS})_{13}|^2, \quad \sin^2 \theta_{23} = \frac{|(U_{PMNS})_{23}|^2}{1 - |(U_{PMNS})_{13}|^2}, \quad \sin^2 \theta_{12} = \frac{|(U_{PMNS})_{12}|^2}{1 - |(U_{PMNS})_{13}|^2}. \quad (\text{II.23})$$

In the model, NH is favored by the structures of Yukawa couplings and Majorana mass matrix. There are two light neutrino masses and one heavy mass.(see appendix A) Therefore the structures naturally realize NH of neutrino masses.

Also, the effective mass for the neutrinoless double beta decay is given by

$$\langle m_{ee} \rangle = |m_{\nu_1} \cos^2 \theta_{12} \cos^2 \theta_{13} + m_{\nu_2} \sin^2 \theta_{12} \cos^2 \theta_{13} e^{i\alpha_{21}} + m_{\nu_3} \sin^2 \theta_{13} e^{i(\alpha_{31} - 2\delta_{CP})}|, \quad (\text{II.24})$$

where its observed value could be measured by KamLAND-Zen in future [47].

## A. Numerical analysis

Here, we demonstrate numerical analysis to find predictions as well as reproduce the current experimental results, where we suppose the DM candidate is an imaginary component of inert scalar  $\eta$ ;  $\eta_I$ , in which we simply assume  $m_{\eta^\pm} \approx m_I$  to evade the oblique parameters. In this case, the mass of DM is within  $534 \pm 8.5$  GeV [48] to satisfy the relic density that arises from the kinetic term only. Here, we work on this range.

Our input parameters are three mass parameters;  $m_R$ ,  $M_0$ ,  $M_1$  and six dimensionless parameters  $\tau$ ,  $\alpha_D$ ,  $\lambda''_{H\eta}$ ,  $\alpha_D$ ,  $\beta_D$ ,  $\gamma_D$ , where we work on the following ranges for both cases:

$$\begin{aligned} \tau &= [-1.5, 1.5] + i[0.5, 2], \quad [|\alpha_D|, \lambda''_{H\eta}] = [1, 10] \times 10^{-7}, \quad [|\alpha_\eta|, |\beta_\eta|, |\gamma_\eta|] = [0.001, 1], \\ m_R &= [525.5, 542.5] \text{ GeV}, \quad M_0 = [10^3, 10^6] \text{ GeV}, \quad M_0 \leq M_1 \leq 10 \times M_0. \end{aligned}$$

Notice here  $m_I = \sqrt{m_R^2 + 2\lambda''_{H\eta} v_H^2}$ , and  $\lambda''_{H\eta}$  is assumed to be a real parameter. Next, we will show some plots in terms of the classification of  $\chi$  square analysis within the range of 1-2 $\sigma$  which is represented by green color, 2-3 $\sigma$  which is represented by yellow color, and 3-5 $\sigma$

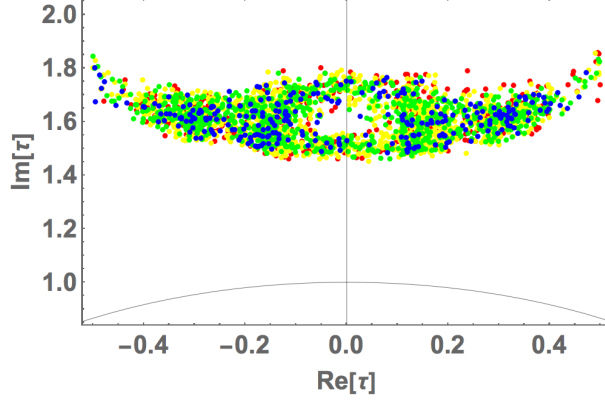


FIG. 1: Allowed region of  $\tau$  in case of NH. In the  $\chi^2$  analysis, the blue color represents  $\leq 1\sigma$ , green 1-2 $\sigma$ , yellow 2-3 $\sigma$ , and red 3-5 $\sigma$ . The black solid line is the boundary of the fundamental domain at  $|\tau| = 1$ .

which is represented by red color, referring to NuFIT 5.0 [49]. In the present work, we adopt the accuracy of  $\chi^2$  for five well known dimensionless observables such as  $\Delta m_{\text{atm}}^2$ ,  $\sin^2 \theta_{23}$ ,  $\sin^2 \theta_{13}$ ,  $\Delta m_{\text{sol}}^2$ , and  $\sin^2 \theta_{12}$ . Notice here that the masses of charged-lepton can precisely be fitted by  $\alpha_\ell, \beta_\ell, \gamma_\ell$ . Thus, we do not include these masses in the  $\chi^2$  analysis.

In case of NH, the lightest  $D_N$  is heavier than 500 TeV. These suggest that they are totally safe for LFV constraints. In case of IH, we need fine-tuned parameters and the LFV processes become very large. Therefore, we would not find any solutions to satisfy the LFV constraint. We will discuss only the case of NH in this section. Fig. 1 shows allowed region of  $\tau$  in the fundamental space, where the blue color represents  $\leq 1\sigma$ , green 1-2 $\sigma$ , yellow 2-3 $\sigma$ , and red 3-5 $\sigma$ .

Fig. 2 shows the sum of neutrino masses  $\sum m_i (\equiv \text{Tr}[D_\nu])$  versus the effective mass for the neutrinoless double beta decay  $\langle m_{ee} \rangle$ , depending on the  $\chi^2$  analysis. The color distribution is the same as the one in Fig. 1. It suggests that  $1 \text{ meV} \lesssim \langle m_{ee} \rangle \lesssim 4 \text{ meV}$  and  $58 \text{ meV} \lesssim \sum m \lesssim 62 \text{ meV}$  within the range of  $5\sigma$ . It implies large neutrino mass hierarchies  $m_{\nu_1} \ll m_{\nu_2} \ll m_{\nu_3}$ , since the sum of masses is close to  $\sqrt{\Delta m_{\text{atm}}^2}$ . Notice here that the total neutrino masses are consistent with the recent cosmological constraint;  $\sum m_i \leq 120 \text{ meV}$ .

Fig. 3 shows correlations among Dirac CP phase  $\delta_{CP}$  and Majorana phases  $\alpha_{21,31}$  in case of NH. The color distribution is the same as the one in Fig. 1. The Dirac CP phase and the



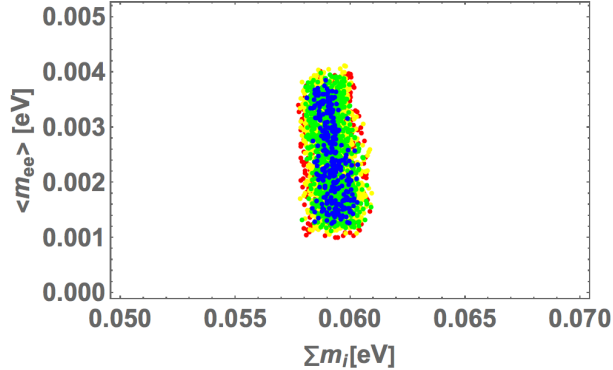


FIG. 2: The sum of neutrino masses  $\sum m_i (\equiv \text{Tr}[D_\nu])$  versus the effective mass for the neutrinoless double beta decay  $\langle m_{ee} \rangle$  in case of NH. The color distribution is the same as the one in Fig. 1.

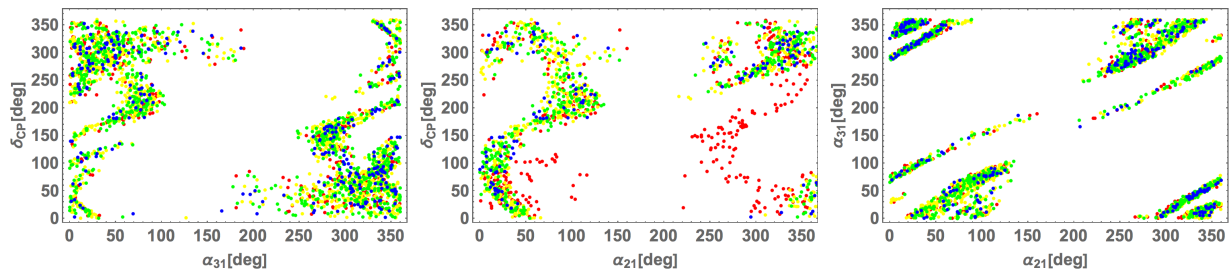


FIG. 3: Correlations among Dirac CP phase  $\delta_{CP}$  and Majorana phases  $\alpha_{21,31}$  in case of NH. The color distribution is the same as the one in Fig. 1.

Majorana phase  $\alpha_{31}$  run over whole the range. The Majorana phase  $\alpha_{21}$  runs over whole the range except around  $180^\circ$ . We show two sample points in Tab. III, where the first one is selected so as to minimize  $\chi^2$ , while the second one is chosen that  $\delta_{CP}^\ell$  be closest value of best fit;  $195^\circ$ . In case of IH we have found allowed region above the range of  $2\sigma$ , but all of the regions are excluded by the constraint of  $\mu \rightarrow e\gamma$ . Thus, we do not show the results in this case.

### III. CONCLUSION AND DISCUSSION

We have explored a predictive lepton model with a modular  $S_4$  symmetry, in which we have generated the neutrino mass matrix at one-loop level. The tree-level mass matrix is forbidden by well-assigned modular weights, which also play an important role in stabilizing

	$\chi = 0.975$	$\chi = 1.54$
$\tau$	$-0.872142 + 1.58675 i$	$-0.927 + 1.75 i$
$[\frac{m_0}{\text{GeV}}, \frac{M_0}{\text{TeV}}, \frac{M_1}{\text{TeV}}]$	[535, 373, 3393]	[ 536, 293, 2601]
$\lambda''_{H\eta}$	$1.44 \times 10^{-7}$	$9.76 \times 10^{-8}$
$[\alpha_\ell, \beta_\ell, \gamma_\ell]$	[0.00102, -0.354, 0.506]	[0.00222, -0.320, 0.523]
$[\alpha_\eta, \gamma_\eta]$	[0.00981 $e^{0.12i}$ , 0.806 $e^{-3.13i}$ ]	[0.00958 $e^{-0.146i}$ , 1.01 $e^{0.0105i}$ ]
$[\beta_{\eta_1}, \beta_{\eta_2}]$	[0.176 $e^{2.24i}$ , 0.455 $e^{-2.95i}$ ]	[0.128 $e^{-2.34i}$ , 0.638 $e^{-0.103i}$ ]
$V_{eL}$	$\begin{pmatrix} 0.325 & -0.108 & -0.940 \\ -0.0570 - 0.270i & -0.1055 - 0.955i & -0.00757 + 0.0163i \\ 0.173 - 0.888i & -0.0765 + 0.243i & 0.0684 - 0.335i \end{pmatrix}$	$\begin{pmatrix} 0.243 & -0.0493 & -0.969 \\ -0.0192 - 0.164i & -0.0506 - 0.985i & -0.00223 + 0.00905i \\ 0.108 - 0.950i & -0.0287 + 0.155i & 0.0284 - 0.246i \end{pmatrix}$
$V_\nu$	$\begin{pmatrix} -0.492 + 0.178i & 0.467 + 0.465i & -0.0362 + 0.539i \\ -0.175 - 0.131i & -0.470 - 0.468i & 0.130 + 0.704i \\ -0.630 + 0.530i & -0.232 - 0.269i & -0.286 - 0.338i \end{pmatrix}$	$\begin{pmatrix} -0.675 + 0.0560i & 0.337 - 0.358i & -0.467 + 0.286i \\ -0.0264 - 0.114i & 0.210 + 0.642i & 0.122 + 0.718i \\ -0.313 + 0.655i & 0.0919 + 0.541i & -0.0671 - 0.408i \end{pmatrix}$
$\sin \theta_{12}$	0.548	0.544
$\sin \theta_{23}$	0.756	0.766
$\sin \theta_{13}$	0.148	0.150
$\delta_{CP}^\ell$	275°	194°
$[\alpha_{21}, \alpha_{31}]$	[251°, 336°]	[313°, 333°]
$\sum m_i$	58.9 meV	58.8 meV
$\langle m_{ee} \rangle$	2.51 meV	3.61 meV

TABLE III: Numerical values of parameters and observables at the sample points of NH.

dark matter candidate due to a remnant  $Z_2$  symmetry even after breaking the modular symmetry. It implies one does not need to impose any additional symmetries such as  $Z_2$  by hand. Embedding three families of the Majorana neutrinos, right-handed charged-leptons and left-handed charged-leptons into singlet, doublet, and triplet respectively under  $S_4$ . We have found allowed regions to satisfy all the relevant experimental constraints and obtained several predictions for NH. While we have not found the allowed region in case of IH, since whole the allowed region to satisfy the neutrino oscillation data conflicts with the constraint of  $\mu \rightarrow e\gamma$ . Then, we have shown our numerical results in figures such as phases, mixings, and neutrino masses, applying  $\chi^2$  analysis. We have also demonstrate two sample points, imposing on minimizing  $\chi^2$  and best fit value of  $\delta_{CP}^\ell$  of 195°. We have found that 1 meV  $\lesssim \langle m_{ee} \rangle \lesssim 4$  meV and 58 meV  $\lesssim \sum m \lesssim 62$  meV within the range of  $5\sigma$ . It suggests that large neutrino mass hierarchies  $m_{\nu_1} \ll m_{\nu_2} \ll m_{\nu_3}$  is realized, since the sum of masses is

close to  $\sqrt{\Delta m_{\text{atm}}^2}$ . Notice here that the total neutrino masses are consistent with the recent cosmological constraint;  $\sum m_i \leq 120$  meV.

## Acknowledgments

*This research was supported by an appointment to the JRG Program at the APCTP through the Science and Technology Promotion Fund and Lottery Fund of the Korean Government. This was also supported by the Korean Local Governments - Gyeongsangbuk-do Province and Pohang City (H.O.). H. O. is sincerely grateful for the KIAS member, and log cabin at POSTECH to provide nice space to come up with this project. Y. O. was supported from European Regional Development Fund-Project Engineering Applications of Microworld Physics (No.CZ.02.1.01/0.0/0.0/16\_019/0000766)*

## Appendix A: Mass structure

$y_i$ 's are given by

$$y_1 = -3\pi \left( \frac{b_1}{8} + 3b_5 \right), \quad (\text{A.1})$$

$$y_2 = 3\sqrt{3}\pi b_3, \quad (\text{A.2})$$

$$y_3 = -\pi \left( -\frac{b_1}{4} + 2b_5 \right), \quad (\text{A.3})$$

$$y_4 = -\pi\sqrt{2}b_2, \quad (\text{A.4})$$

$$y_5 = -4\pi\sqrt{2}b_4, \quad (\text{A.5})$$

where  $b_i$  are given by

$$b_1 \sim 1, \quad b_2 \sim q, \quad b_3 \sim q^2, \quad b_4 \sim 0, \quad b_5 \sim 0, \quad (\text{A.6})$$

with  $q = \exp(2\pi i\tau)$  and  $|q| \ll 1$  [39].

The structures of the majorana mass matrix and the yukawa coupling  $y_\eta$  is written by

$$M_N = M_0 \begin{bmatrix} \mathcal{O}(q^0) & \mathcal{O}(q^2) & \mathcal{O}(q^0) \\ \mathcal{O}(q^2) & \mathcal{O}(q^0) & \mathcal{O}(q^2) \\ \mathcal{O}(q^0) & \mathcal{O}(q^2) & 0 \end{bmatrix}, \quad (\text{A.7})$$

$$y_\eta = \begin{bmatrix} \mathcal{O}(q^2) & \mathcal{O}(q^0) & \mathcal{O}(q^2) \\ \mathcal{O}(q^1) & \mathcal{O}(q^3) & \mathcal{O}(q^1) \\ \mathcal{O}(q^3) & \mathcal{O}(q^1) & \mathcal{O}(q^3) \end{bmatrix}, \quad (\text{A.8})$$

where we assume  $M_0 \sim M_1$ . Using Eq.(A.7), (A.8) and (II.19), we can obtain the neutrino mass structure as following:

$$m_\nu = \begin{bmatrix} \mathcal{O}(q^0) & \mathcal{O}(q^3) & \mathcal{O}(q^1) \\ \mathcal{O}(q^3) & \mathcal{O}(q^2) & \mathcal{O}(q^4) \\ \mathcal{O}(q^1) & \mathcal{O}(q^4) & \mathcal{O}(q^2) \end{bmatrix}. \quad (\text{A.9})$$

Two eigenvalues of  $m_\nu$  are proportional to  $q^2$  and one is proportional to  $q^0$ . It means that the model has two light neutrino masses and one heavy mass.

## Appendix B: Confidence level

We discuss the calculation of the CL.

The probability density function is written by the following form:

$$f(x, \nu) = \frac{x^{\nu/2-1} \exp(-\frac{x}{2})}{2^{\nu/2} \Gamma(\frac{\nu}{2})}, \quad (\text{B.1})$$

where  $\nu$  is the degree of freedom (DOF). It is normalized by

$$\int_0^\infty f(x, \nu) dx = 1. \quad (\text{B.2})$$

The CL for  $\nu$  DOF is given by

$$\int_0^{\Delta\chi^2} f(x, \nu) dx, \quad (\text{B.3})$$

where  $\Delta\chi^2 = \sum_{i=1}^\nu (\chi_i^2 - \chi_{i,min}^2)$  and all parameters are independent. We can get the values  $\chi_i^2$  and  $\chi_{i,min}^2$  from NuFIT 5.0 [49].

Tab. IV shows values  $\Delta\chi^2$  corresponding to CL for joint estimation of  $\nu$  parameters.

- 
- [1] E. Ma, Phys. Rev. D **73**, 077301 (2006) doi:10.1103/PhysRevD.73.077301 [hep-ph/0601225].  
[2] R. de Adelhart Toorop, F. Feruglio and C. Hagedorn, Nucl. Phys. B **858**, 437 (2012) [arXiv:1112.1340 [hep-ph]].

CL(%)	$\nu = 1$	$\nu = 2$	$\nu = 3$	$\nu = 4$	$\nu = 5$	$\nu = 6$
68.27 ( $1\sigma$ )	1.00	2.30	3.53	4.72	5.89	7.04
95.45 ( $2\sigma$ )	4.00	6.18	8.02	9.72	11.31	12.85
99.73 ( $3\sigma$ )	9.00	11.83	14.16	16.25	18.21	20.06
$100 - 5.7 \times 10^{-5}$ ( $5\sigma$ )	25.00	28.74	31.81	34.56	37.09	39.49

TABLE IV: Values  $\Delta\chi^2$  corresponding to CL for joint estimation of  $\nu$  parameters.

- [3] F. Feruglio, doi:10.1142/9789813238053\_0012 arXiv:1706.08749 [hep-ph].
- [4] J. C. Criado and F. Feruglio, arXiv:1807.01125 [hep-ph].
- [5] T. Kobayashi, N. Omoto, Y. Shimizu, K. Takagi, M. Tanimoto and T. H. Tatsuishi, JHEP **1811**, 196 (2018) doi:10.1007/JHEP11(2018)196 [arXiv:1808.03012 [hep-ph]].
- [6] H. Okada and M. Tanimoto, Phys. Lett. B **791**, 54 (2019) doi:10.1016/j.physletb.2019.02.028 [arXiv:1812.09677 [hep-ph]].
- [7] T. Nomura and H. Okada, arXiv:1904.03937 [hep-ph].
- [8] H. Okada and M. Tanimoto, arXiv:1905.13421 [hep-ph].
- [9] F. J. de Anda, S. F. King and E. Perdomo, arXiv:1812.05620 [hep-ph].
- [10] P. P. Novichkov, S. T. Petcov and M. Tanimoto, arXiv:1812.11289 [hep-ph].
- [11] T. Nomura and H. Okada, arXiv:1906.03927 [hep-ph].
- [12] H. Okada and Y. Orikasa, arXiv:1907.13520 [hep-ph].
- [13] T. Nomura, H. Okada and O. Popov, arXiv:1908.07457 [hep-ph].
- [14] T. Kobayashi, K. Tanaka and T. H. Tatsuishi, Phys. Rev. D **98** (2018) no.1, 016004 [arXiv:1803.10391 [hep-ph]].
- [15] T. Kobayashi, Y. Shimizu, K. Takagi, M. Tanimoto, T. H. Tatsuishi and H. Uchida, Phys. Lett. B **794**, 114 (2019) doi:10.1016/j.physletb.2019.05.034 [arXiv:1812.11072 [hep-ph]].
- [16] T. Kobayashi, Y. Shimizu, K. Takagi, M. Tanimoto and T. H. Tatsuishi, arXiv:1906.10341 [hep-ph].
- [17] H. Okada and Y. Orikasa, arXiv:1907.04716 [hep-ph].
- [18] J. T. Penedo and S. T. Petcov, Nucl. Phys. B **939**, 292 (2019) doi:10.1016/j.nuclphysb.2018.12.016 [arXiv:1806.11040 [hep-ph]].
- [19] P. P. Novichkov, J. T. Penedo, S. T. Petcov and A. V. Titov, JHEP **1904**, 005 (2019)

- doi:10.1007/JHEP04(2019)005 [arXiv:1811.04933 [hep-ph]].
- [20] T. Kobayashi, Y. Shimizu, K. Takagi, M. Tanimoto and T. H. Tatsuishi, arXiv:1907.09141 [hep-ph].
- [21] P. P. Novichkov, J. T. Penedo, S. T. Petcov and A. V. Titov, arXiv:1812.02158 [hep-ph].
- [22] G. J. Ding, S. F. King and X. G. Liu, arXiv:1903.12588 [hep-ph].
- [23] A. Baur, H. P. Nilles, A. Trautner and P. K. S. Vaudrevange, arXiv:1901.03251 [hep-th].
- [24] G. J. Ding, S. F. King, C. C. Li and Y. L. Zhou, *JHEP* **08**, 164 (2020) doi:10.1007/JHEP08(2020)164 [arXiv:2004.12662 [hep-ph]].
- [25] I. de Medeiros Varzielas, S. F. King and Y. L. Zhou, arXiv:1906.02208 [hep-ph].
- [26] X. G. Liu and G. J. Ding, arXiv:1907.01488 [hep-ph].
- [27] G. Altarelli and F. Feruglio, *Rev. Mod. Phys.* **82** (2010) 2701 [arXiv:1002.0211 [hep-ph]].
- [28] H. Ishimori, T. Kobayashi, H. Ohki, Y. Shimizu, H. Okada and M. Tanimoto, *Prog. Theor. Phys. Suppl.* **183** (2010) 1 [arXiv:1003.3552 [hep-th]].
- [29] H. Ishimori, T. Kobayashi, H. Ohki, H. Okada, Y. Shimizu and M. Tanimoto, *Lect. Notes Phys.* **858** (2012) 1, Springer.
- [30] D. Hernandez and A. Y. Smirnov, *Phys. Rev. D* **86** (2012) 053014 [arXiv:1204.0445 [hep-ph]].
- [31] S. F. King and C. Luhn, *Rept. Prog. Phys.* **76** (2013) 056201 [arXiv:1301.1340 [hep-ph]].
- [32] S. F. King, A. Merle, S. Morisi, Y. Shimizu and M. Tanimoto, arXiv:1402.4271 [hep-ph].
- [33] S. F. King, *Prog. Part. Nucl. Phys.* **94** (2017) 217 doi:10.1016/j.pnpnp.2017.01.003 [arXiv:1701.04413 [hep-ph]].
- [34] S. T. Petcov, *Eur. Phys. J. C* **78** (2018) no.9, 709 [arXiv:1711.10806 [hep-ph]].
- [35] A. Baur, H. P. Nilles, A. Trautner and P. K. S. Vaudrevange, arXiv:1908.00805 [hep-th].
- [36] M. Hirsch, S. Morisi, E. Peinado and J. W. F. Valle, *Phys. Rev. D* **82**, 116003 (2010) doi:10.1103/PhysRevD.82.116003 [arXiv:1007.0871 [hep-ph]].
- [37] J. M. Lamprea and E. Peinado, *Phys. Rev. D* **94**, no. 5, 055007 (2016) doi:10.1103/PhysRevD.94.055007 [arXiv:1603.02190 [hep-ph]].
- [38] L. M. G. De La Vega, R. Ferro-Hernandez and E. Peinado, *Phys. Rev. D* **99**, no. 5, 055044 (2019) doi:10.1103/PhysRevD.99.055044 [arXiv:1811.10619 [hep-ph]].
- [39] P. P. Novichkov, J. T. Penedo, S. T. Petcov and A. V. Titov, arXiv:1905.11970 [hep-ph].
- [40] S. Baek, T. Nomura and H. Okada, *Phys. Lett. B* **759**, 91 (2016) doi:10.1016/j.physletb.2016.05.055 [arXiv:1604.03738 [hep-ph]].

- [41] M. Lindner, M. Platscher and F. S. Queiroz, *Phys. Rept.* **731**, 1 (2018) doi:10.1016/j.physrep.2017.12.001 [arXiv:1610.06587 [hep-ph]].
- [42] A. M. Baldini *et al.* [MEG Collaboration], *Eur. Phys. J. C* **76**, no. 8, 434 (2016) [arXiv:1605.05081 [hep-ex]].
- [43] F. Renga [MEG Collaboration], *Hyperfine Interact.* **239**, no. 1, 58 (2018) [arXiv:1811.05921 [hep-ex]].
- [44] B. Aubert *et al.* [BaBar Collaboration], *Phys. Rev. Lett.* **104** (2010) 021802 [arXiv:0908.2381 [hep-ex]].
- [45] N. Aghanim *et al.* [Planck Collaboration], arXiv:1807.06209 [astro-ph.CO].
- [46] S. Vagnozzi, E. Giusarma, O. Mena, K. Freese, M. Gerbino, S. Ho and M. Lattanzi, *Phys. Rev. D* **96**, no. 12, 123503 (2017) doi:10.1103/PhysRevD.96.123503 [arXiv:1701.08172 [astro-ph.CO]].
- [47] A. Gando *et al.* [KamLAND-Zen Collaboration], *Phys. Rev. Lett.* **117**, no. 8, 082503 (2016) Addendum: [*Phys. Rev. Lett.* **117**, no. 10, 109903 (2016)] doi:10.1103/PhysRevLett.117.109903, 10.1103/PhysRevLett.117.082503 [arXiv:1605.02889 [hep-ex]].
- [48] T. Hambye, F.-S. Ling, L. Lopez Honorez and J. Rocher, *JHEP* **0907**, 090 (2009) Erratum: [*JHEP* **1005**, 066 (2010)] doi:10.1007/JHEP05(2010)066, 10.1088/1126-6708/2009/07/090 [arXiv:0903.4010 [hep-ph]].
- [49] I. Esteban, M. C. Gonzalez-Garcia, M. Maltoni, T. Schwetz and A. Zhou, *JHEP* **09**, 178 (2020) doi:10.1007/JHEP09(2020)178 [arXiv:2007.14792 [hep-ph]].
- [50] K. Abe *et al.* [T2K Collaboration], *Phys. Rev. Lett.* **121**, no. 17, 171802 (2018) doi:10.1103/PhysRevLett.121.171802 [arXiv:1807.07891 [hep-ex]].
- [51] P. Adamson *et al.* [NOvA Collaboration], *Phys. Rev. Lett.* **118**, no. 23, 231801 (2017) doi:10.1103/PhysRevLett.118.231801 [arXiv:1703.03328 [hep-ex]].